

Figure 1: Pilot-aided SLM based OFDM system model

of SI is an overhead on the data and thus reduces data throughput. Furthermore, successful detection of SI may add to the design complexity of the receiver. In the literature, some methods which perform SI estimation without the need for SI transmission have been proposed, however they require increased complexity of implementation and also rely on statistical methods of detection [20, 21, 24, 25].

In contrast to randomly generated sequences chosen from $\{\pm 1, \pm j\}$ as suggested in [17], binary sequences chosen from the set $\{\pm 1\}$ were shown to be adequate for reducing PAPR and are recommended in [26] for SLM based OFDM systems because they offer simpler implementation. Binary sequences have two unique phases i.e. 0 and π . Chaotic-Binary (CB) [27], Shapiro-Rudin (SR) [28] and Hadamard [29] sequences are common examples of binary sequences. Discussions in both [27] and [30] suggest that CB sequences have improved PAPR reduction capability over SR and Hadamard sequences. However, construction of CB sequences requires a significant number of Digital Signal Processor (DSP) computations. As a consequence, CB sequences therefore consume more power and may actually cancel the quantity of power saved as a result of reducing PAPR.

In an attempt to create alternative binary sequences with relatively lower computational complexity, this paper presents a form of binary sequences called Fibonacci-Binary sequences which are derived

from a Fibonacci series. In this paper simulations are undertaken to compare CB and Fibonacci-Binary sequences in terms of computational complexity, PAPR reduction performance and in the presence of some pre-defined levels of non-linear PA distortion, the BER performance in a multipath fading channel condition.

The paper is structured as follows. Section 2 describes the SLM based OFDM system model used for the simulation investigations within this paper. Section 3 presents the method for constructing CB sequences and section 4 describes the construction of the proposed Fibonacci-Binary sequences. Section 5 presents the results and discussions related PAPR reduction, BER performance and computational complexity between both forms of binary sequences. Finally, conclusions based on the outcomes of the paper are presented in section 6.

2 System Model: SLM Based OFDM

This section provides a brief description of the SLM based OFDM system used in the investigations. The block diagram of the SLM based OFDM system is shown in Figure 1.

Let x_n represent an OFDM signal for $0 \leq n \leq (N - 1)$ where N is the size of an inverse fast Fourier transform (IFFT). The PAPR of x_n is defined by the ratio

$$PAPR\{x_n\} = \frac{\max \{|x_n|^2\}}{E\{|x_n|^2\}} \quad (1)$$

where $E\{\cdot\}$ represents the expectation function and x_n is expressed by

$$\begin{aligned} x_n &= \frac{1}{\sqrt{N}} \sum_{k=0}^{N_v-1} X[k] \exp(j2\pi nk/N) \\ &= IFFT\{X[k]\} \end{aligned} \quad (2)$$

In (2), k represents the subcarrier index for $0 \leq k \leq (N_v - 1)$, N_v is the number of subcarriers in the OFDM sequence $X[k]$ and $IFFT$ is the IFFT function. Normally $N_v < N$ and the value of N is usually a power of 2 to permit a radix-2 [31] or split-radix [32] IFFT implementation. Hence, when $N > N_v$, a zero padded IFFT may be used. Let $X[k]$ represent a pilot-aided OFDM sequence consisting of N_p pilot and N_d data subcarrier components such that $N_v = N_p + N_d$. Let l represent an arbitrary index for the allocation of each subcarrier symbol within the range $0 \leq l \leq (L - 1)$, where L is defined as the pilot spacing i.e. the number of subcarriers separating two consecutive pilot symbols. Then, according to the data-pilot arrangement depicted in Figure 2, each subcarrier element $X[k]$ may be represented as follows:

$$\begin{aligned} X[k] &= X[mL + l] \text{ for } 0 \leq m \leq N_p - 1 \\ &= \begin{cases} X_p[m], & l = 0 \\ X_d[mL + l], & \text{otherwise} \end{cases} \end{aligned} \quad (3)$$

where m represents an arbitrary index for pilot allocation, and $X_p[m]$ and $X_d[mL + l]$ respectively denote each individual pilot and data subcarrier symbol.

Let U equal the number of SLM sequence vectors or modified OFDM signals. In addition, let $B^u[k]$ represent each SLM sequence vector for $0 \leq u \leq (U - 1)$, where the superscript u represents the sequence vector index. SLM thus creates multiple OFDM signals x_n^u as represented by

$$x_n^u = IFFT\{X^u[k]\} \text{ where } X^u[k] = X[k] \cdot B^u[k] \quad (4)$$

One of the SLM sequence vectors, denoted by $B^{\bar{u}}[k]$,

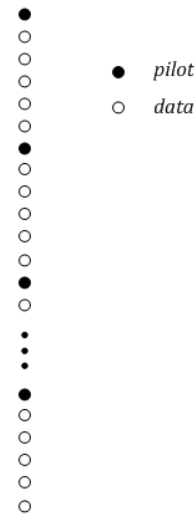


Figure 2: Representation of the data-pilot allocation within multi subcarrier OFDM symbol transmissions

will be the optimum sequence vector that produces the selected signal $x_n^{\bar{u}}$ with the lowest PAPR. The value \bar{u} is often termed the SI which must be accurately known at the receiver for successful identification of the relevant SLM vector sequence that produces the transmitted signal. Hence, accurate knowledge of \bar{u} is important to achieve successful data recovery. Similar to $X[k]$, data and pilot components of $B^{\bar{u}}[k]$ are denoted by $B_d^{\bar{u}}[mL + l]$ and $B_p^{\bar{u}}[m]$ respectively.

As is normal in OFDM systems, the length of $x_n^{\bar{u}}$ is further extended by cyclic prefixing (CP) as described in [33]. CP provides a guard interval (GI) between consecutive OFDM transmissions and in order to prevent poor data recovery due to channel induced inter-symbol interference (ISI), the GI duration must be greater than the maximum delay τ_{max} of the transmission channel.

At the receiver, CP samples are first removed before transforming the received OFDM time domain signal into the OFDM frequency domain sequence, denoted by $\bar{Y}[k]$, through application of the fast Fourier transform (FFT). After the FFT stage, the OFDM sequence $\bar{Y}[k]$ is expressed by

$$\bar{Y}[k] = H[k]X[k]B^{\bar{u}}[k] + V[k] \quad (5)$$

where $H[k]$ and $V[k]$ represent the channel gain and additive white Gaussian noise (AWGN) of the k^{th} subcarrier symbol. Similar to $X[k]$, pilot components of $H[k]$ and $\bar{Y}[k]$ are respectively represented by $H_p[m]$ and $\bar{Y}_p[m]$ while the data components are denoted by $H_d[mL + l]$ and $\bar{Y}_d[mL + l]$. For data

recovery, let \hat{u} represents the SI estimate. Assuming perfect SI detection i.e. $\hat{u} = \bar{u}$, then data decoding can be obtained using a form of Maximum-Likelihood (ML) detection represented as follows:

$$\hat{X}_d[mL+l] = \min_{Q[q] \in \mathbb{Q}} |Y_d[mL+l] - \hat{H}_d[mL+l]Q[q]|^2 \quad (6)$$

where $Y_d[mL+l] = \bar{Y}_d[mL+l]B_d^{\hat{u}}[mL+l]^*$, \mathbb{Q} is a set of Q constellation points of the chosen data modulation scheme, $\hat{X}_d[mL+l] \in \mathbb{Q}$, $1 \leq q \leq Q$, and $\hat{H}_d[mL+l]$ is the data sub-channel estimate obtained by linear interpolation between values of the pilot sub-channel estimates $\hat{H}_p[m]$, given by

$$\hat{H}_p[m] = Y_p[m]/X_p[m] \quad (7)$$

where $Y_p[m] = \bar{Y}_p[m]B_p^{\hat{u}}[m]^*$.

3 Chaotic-Binary Sequences

This section describes the method of constructing CB sequences from a chaotic system normally described by a logistic map i.e. an iterative equation, as outlined in [27]. The state or the point at which a chaotic system becomes chaotic is highly sensitive to the initial conditions of the system. Examples of practical applications where chaotic sequences have been used include compressive sensing [34] and direct-sequence spread spectrum for multiple access schemes [35,36].

CB sequences are derived from an iterative equation and then transformed into a binary sequence with elements chosen from the set $\{\pm 1\}$. These produce 0 and π phase shifts which are applied in SLM to each subcarrier symbol for reducing PAPR. A form of chaotic sequences which consists of real-valued elements has also been suggested and applied to reduce PAPR [37, 38]. However, this form of real-valued chaotic sequences usually results in depreciated BER degradation since real-valued sequences modify both amplitudes and phases of subcarrier symbols when applied in SLM schemes. As a result, CB sequences applied to the phases of OFDM symbols are preferred in SLM schemes as demonstrated in [27].

As outlined in [27], CB sequences can be constructed from an iterative equation defined by

$$c_{i+1} = 1 - 2c_i^2 \quad (8)$$

where $c_0 \notin (\pm 0.5)$ and $c_0 \in (-1, 1)$. In this paper, c_0 is set to 0.1. For $0 \leq i \leq (N_v - 1)$, an $(N_v \times 1)$ CB vector is formed by transformation of c_i i.e.

$$C_i = \text{sgn}(c_i) \quad (9)$$

where $\text{sgn}(\cdot)$ is the signum function and $C_i \in \{\pm 1\}$. The required U CB sequence vectors are then formed by circular shifting of C_i .

4 Proposed: Fibonacci Binary Polynomial Sequences

This section presents the method of constructing an alternative set of binary sequences referred to as Fibonacci-Binary (FB) sequences using the numbers in a Fibonacci series. The Fibonacci series was first introduced in 1202 by Leonardo Fibonacci [39] and has been applied in various subject areas including geometry [39], mathematics, art, architectural designs and search algorithms [40] [41].

The Fibonacci series is a sequence of integers given by

$$\begin{aligned} F_n &= F_{n-1} + F_{n-2} \\ &= 0, 1, 1, 2, 3, 5, 8, 13, 21, 34 \dots \end{aligned} \quad (10)$$

where $F_0 = 0$, $F_1 = 1$ and $F_n = 0$ for $n < 0$. Using the numbers obtained from (10), the proposed FB sequences are constructed as follows:

Step 1: First, define the required number of terms W to be selected from F_n to form F_W . As an example, if $W = 9$, then

$$F_W = [0, 1, 1, 2, 3, 5, 8, 13, 21] \quad (11)$$

Step 2: Re-arrange the selected numbers in descending order to form \bar{F}_W . As an example, if $W = 9$, then

$$\bar{F}_W = [21, 13, 8, 5, 3, 2, 1, 1, 0] \quad (12)$$

Step 3: Let the numbers in \bar{F}_W represent coefficients of what may be called a Fibonacci polynomial, then by removing one of the 1s since each coefficient of a polynomial must be unique, F_W is reduced to

$$\begin{aligned} \bar{F}_W &= [21, 13, 8, 5, 3, 2, 1, 0] \\ &= x^{21} + x^{13} + x^8 + x^5 + x^3 + x^2 + x + 1 \end{aligned} \quad (13)$$

Table 1: Resulting binary vectors for CB and FB sequences (from step 4) for W set to 8, 9 and 10

Terms	Polynomial	Binary Vector (step 4)
\bar{F}_8	$x^{13} + x^8 + x^5 + x^3 + x^2 + x + 1$	-11111 - 111 - 11 - 1 - 1 - 1 - 1
\bar{F}_9	$x^{21} + x^{13} + x^8 + x^5 + x^3 + x^2 + x + 1$	-11111111 - 11111 - 111 - 11 - 1 - 1 - 1 - 1
\bar{F}_{10}	$x^{34} + x^{21} + x^{13} + x^8 + x^5 + x^3 + x^2 + x + 1$	-11111111111111 - 11111111 - 11111 - 111 ... -11 - 1 - 1 - 1 - 1 - 1

Step 4: The bit representation of \bar{F}_W in (13) can be written as

$$\bar{F}_W = [1000000010000100101111] \quad (14)$$

By replacing 0s and 1s in (14) with +1 and -1 respectively, a binary vector is formed. Table 1 shows resulting Fibonacci polynomial and corresponding binary vector when W is set to 8, 9 and 10.

Step 5: To obtain FB sequences of size $(N_v \times U)$, the resulting binary vector from step 4 is repeatedly cyclic shifted until the number of elements is $\geq (N_v \times U)$

(expressed in dB) is represented by

$$IBO(dB) = 10 \log_{10} \left(\frac{P_{sat}}{P_{avg}} \right) \quad (16)$$

where P_{sat} and P_{avg} denote the PA input saturation power and mean power of the input signal respectively.

Simulations consider a solid state PA (SSPA), often used in mobile communication systems [42] with AM/AM conversion (with unity gain) described by Rapp's model [43], i.e.

$$y(t) = \frac{x(t)}{\left[1 + \left(\frac{|x(t)|}{A_{sat}} \right)^{2\rho} \right]^{1/2\rho}} \quad (17)$$

where $x(t)$ represents the input signal into the SSPA, $y(t)$ is the output signal from the SSPA, A_{sat} is the SSPA output saturation magnitude and ρ is the smoothing factor which controls the PA's transition from linear to saturation region.

5 Simulation Results and Comparison of Computational Complexity

The first aspect of results are obtained from Matlab simulations carried out to evaluate and compare the PAPR reduction and BER performance of the pilot-aided SLM based OFDM system. The second part presents a comparison of computational complexity associated with the construction of CB sequences and the proposed FB sequences. These FB sequences are constructed with W set to 9.

The well known complementary cumulative distribution function (CCDF) is the chosen metric for evaluating the PAPR reduction performance. CCDF gives the probability of a calculated PAPR value $PAPR$ (dB) exceeding a certain threshold γ dB level. The CCDF is thus defined [11] as

$$CCDF\{\gamma\} = Prob(PAPR > \gamma) \quad (15)$$

After transmission over a multipath fading channel and assuming the SI is known, the BER is evaluated in the presence of some pre-defined levels of PA distortion defined by the IBO parameter. The IBO

5.1 Results and Discussion

Simulations consider OFDM transmission over the well known 6-tap COST 207 rural-area (cost207RA) [44] multipath fading channel with $\tau_{max} = 500$ ns for an OFDM system with subcarrier spacing of 15 KHz, sampling frequency of 7.68 MHz, guard interval of 5.21 μ s and $[N, N_v, N_p$ and $L]$ set to [1024, 600, 100 and 6] respectively. The data is modulated using 16-QAM and the pilots modulated using QPSK Gold code sequences. For each SNR value, the number of transmitted OFDM symbols is 40,000. All CCDF curves are evaluated using (360,000) transmitted OFDM symbols.

Figure 3 shows the resulting CCDF curves as a function of γ (dB) from the application of CB sequences and the proposed FB sequences when U is set to 8 and 32. Results in Figure 3 show that when compared to CB sequences, the proposed FB

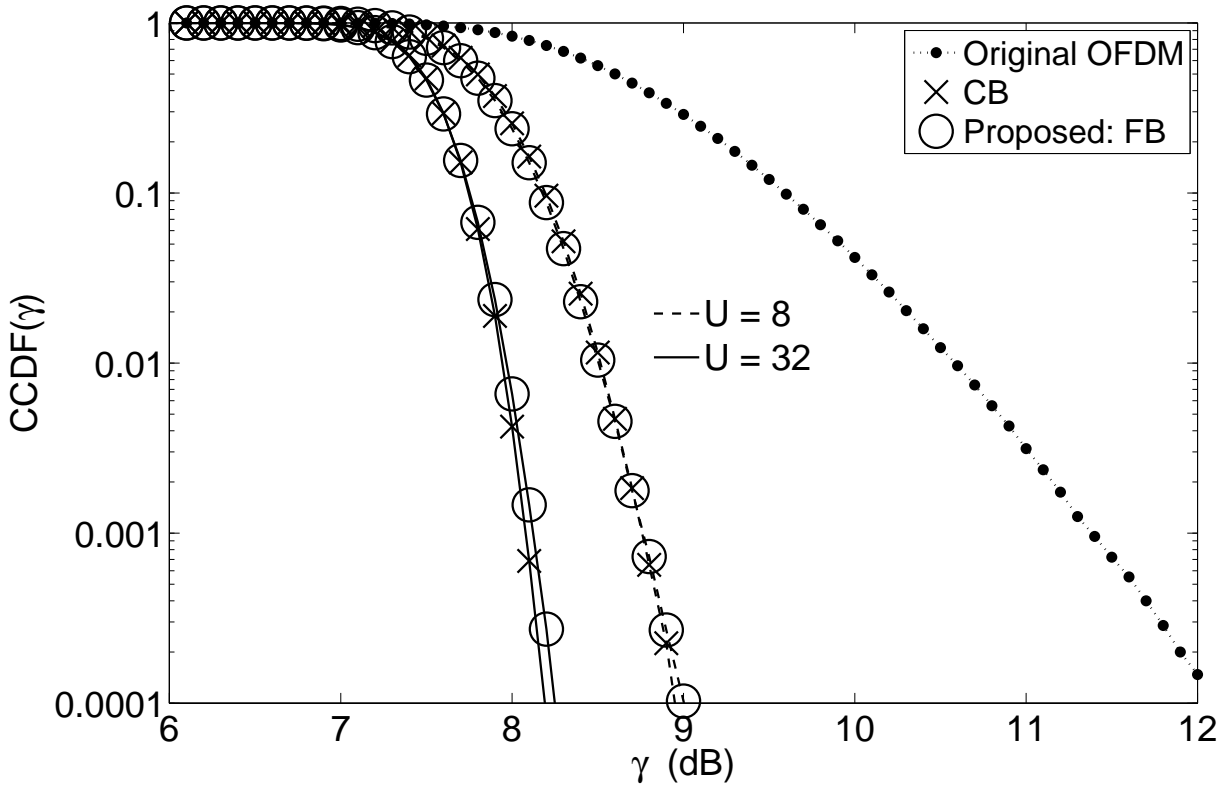


Figure 3: Comparison of CCDF curves for SLM based OFDM system using CB and FB sequences with $U = 8$ and 32

sequences produce slightly less but comparable PAPR reduction performance when $U = 32$ and produce similar PAPR reduction when $U = 8$ at higher CCDF level e.g. 10^{-3} . This is because a slightly higher level of randomness of elements from CB sequences exist when U is large. Numerically, comparison of PAPR reduction performance between the considered forms of binary sequences may be determined by evaluating $\Delta\gamma$ which represents an estimated PAPR reduction gain i.e. the difference between the PAPR values of the original OFDM signal and the SLM based OFDM signal at a given CCDF probability level. Thus, $\Delta\gamma$ (dB) may be calculated as

$$\Delta\gamma = \gamma_{OFDM} - \gamma_{SLM}^{\bar{u}} \tag{18}$$

where γ_{OFDM} and $\gamma_{SLM}^{\bar{u}}$ are the PAPR values of the original OFDM signals and SLM-OFDM signals respectively at the same CCDF probability level. Table 2 displays the calculated values of $\Delta\gamma$ for CB sequences and FB sequences at CCDF probability levels of 10^{-4} and 10^{-3} . These CCDF values were evaluated using simple linear interpolation between the two determined CCDF curve points encompassing the relevant CCDF probability level. This table shows that

Table 2: Comparison of $\Delta\gamma$ (dB) between CB and FB SLM sequences for $W = 9$.

CCDF Level and U	$\Delta\gamma$ (dB)	
	CB	Proposed: FB
10^{-3} $U = 8$	2.600	2.600
10^{-3} $U = 32$	3.300	3.201
10^{-4} $U = 8$	3.200	3.100
10^{-4} $U = 32$	4.000	3.900

for $U = 32$, CB sequences produce a slightly improved PAPR reduction i.e. ≈ 0.1 dB gain over FB sequences but both produce very similar PAPR reduction performance when $U = 8$ and at slightly higher CCDF level of 10^{-3} . This difference though measurable, is to all intents and purposes a very small PAPR difference.

With IBO set to pre-define values of [2 dB, 4 dB and 6 dB], Figures 4 and 5 show comparison of BER curves with ρ set to 2 and 3 respectively when $U = 32$. Results in Figures 4 and 5 show that despite the

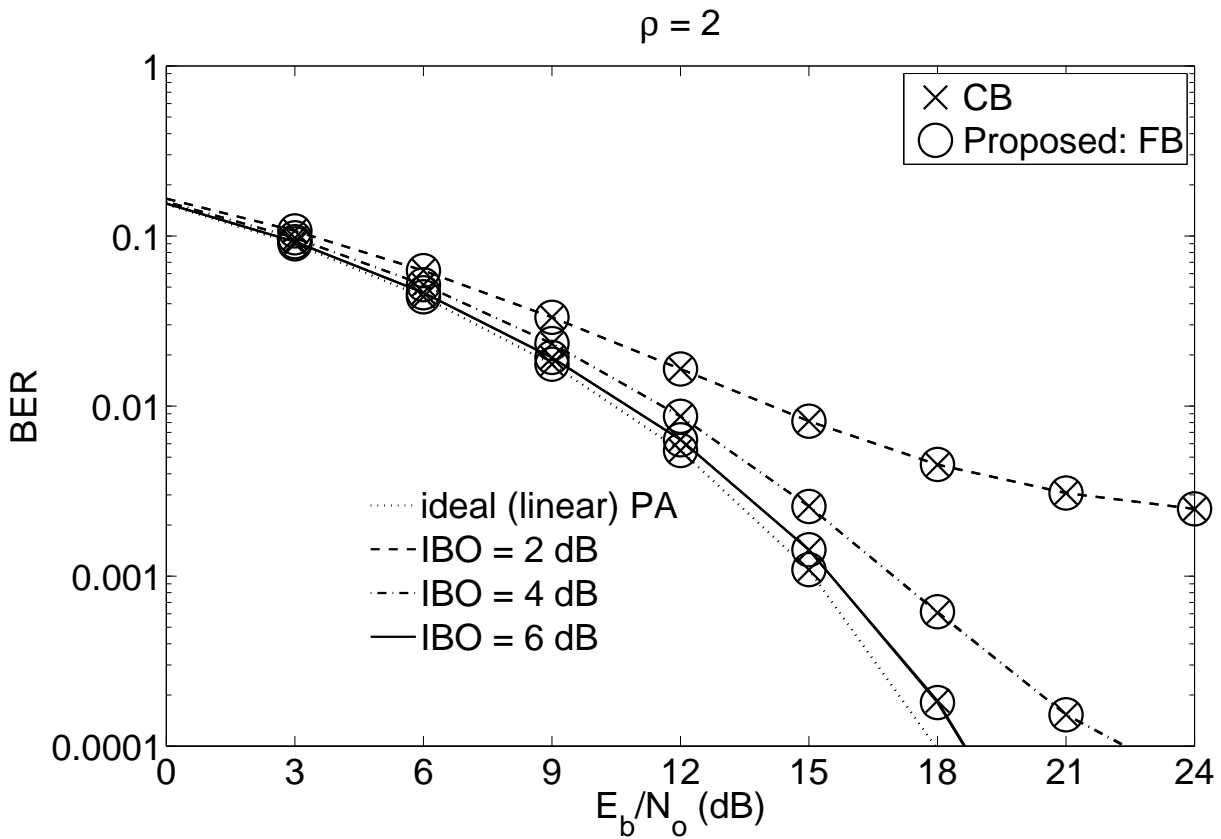


Figure 4: Comparison of BER as a function of IBO for standard OFDM, CB and FB SLM sequences with $\rho = 2$ and $U = 32$

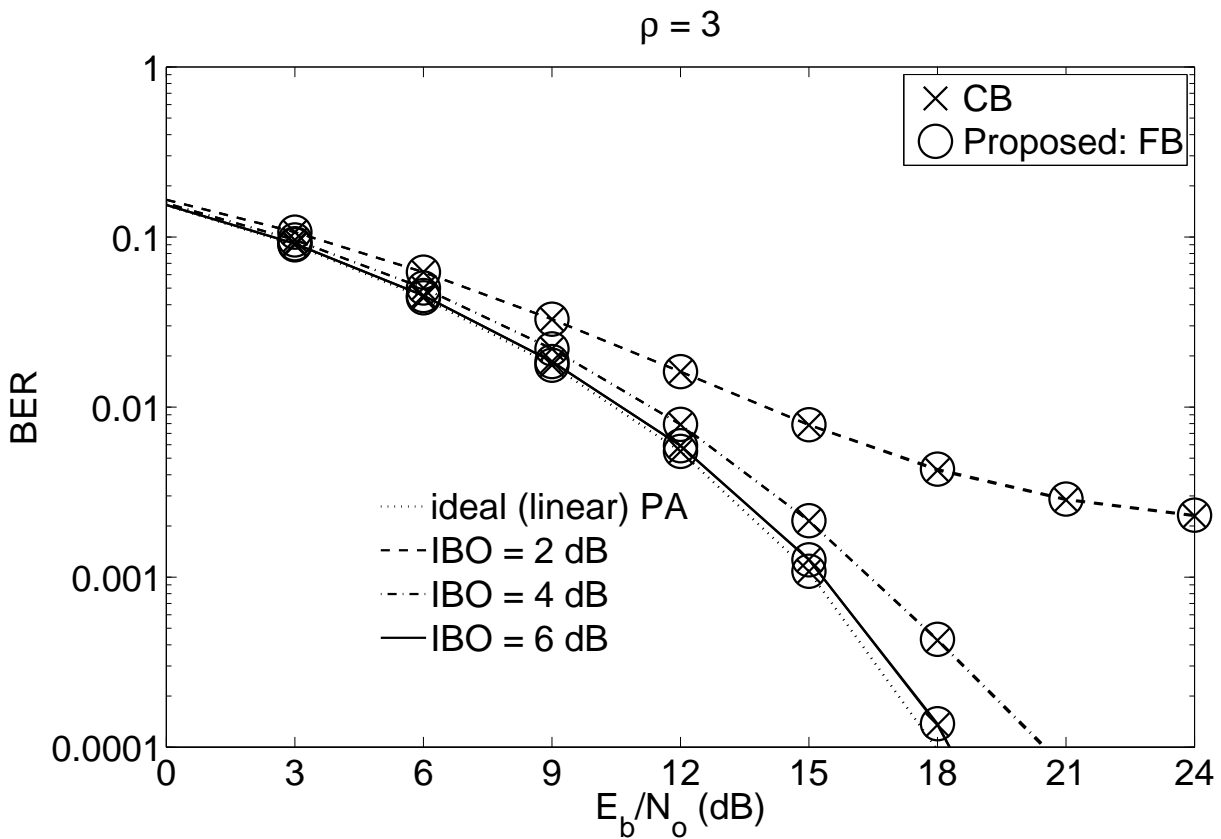


Figure 5: Comparison of BER as a function of IBO for standard OFDM, CB and FB SLM sequences with $\rho = 3$ and $U = 32$

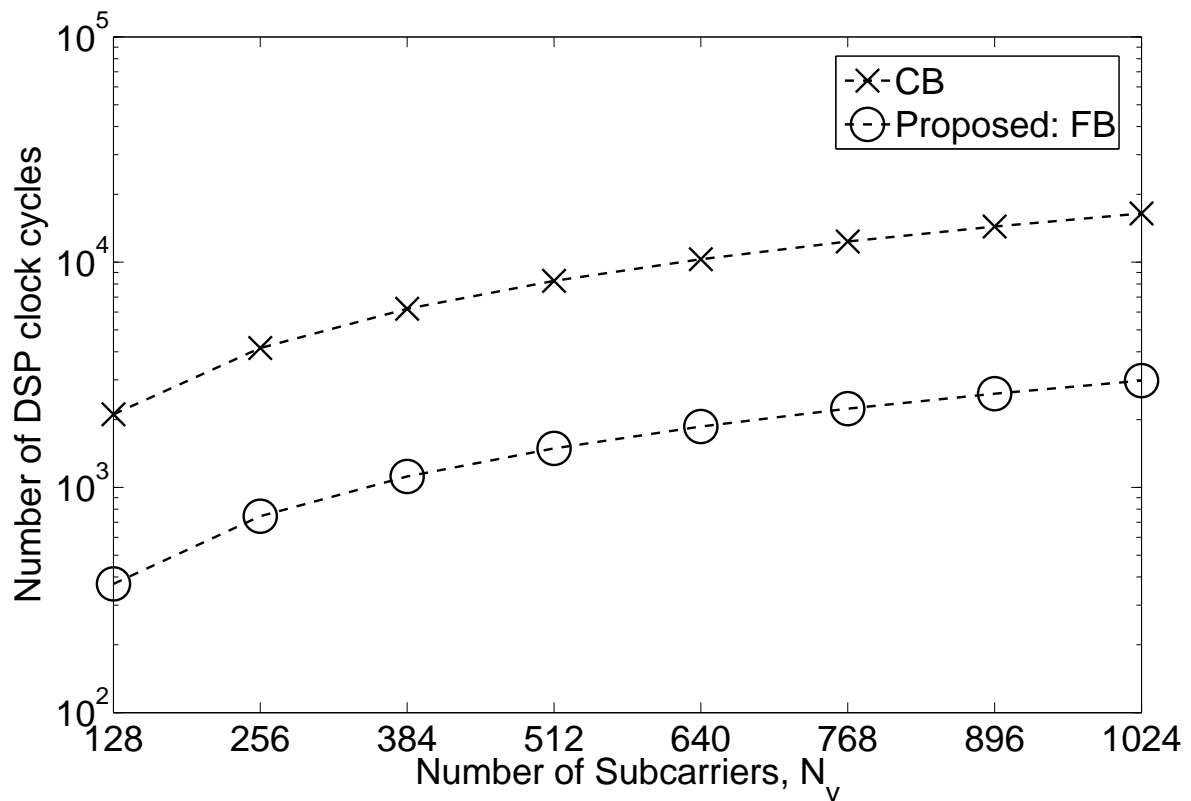


Figure 6: DSP complexity (clock cycles) vs. N_v for implementation of CB and FB SLM sequences

small difference in the PAPR reduction performance of CB and the proposed FB sequences for $U = 32$, both types of sequences produce the same data recovery performance even when some pre-defined levels of non-linear distortion are considered. These results indicate that a small difference in the PAPR reduction performance does not translate to BER degradation for each of the IBO levels considered.

5.2 Comparison of Computational Complexity

In this section, the computational complexity involved in the construction of CB and FB sequences are discussed to demonstrate one of the key advantages of the proposed FB sequences when implemented on a DSP.

From the discussions in section 3, the construction of CB sequences through the expressions in (8) and (9) require $2N_v$ floating point multiplications, $2(U - 1)$ bit-level operations and N_v floating point additions and compare operations. From section 4, assuming the binary vector \bar{F}_W in (14) is pre-determined, then construction of FB sequences i.e. step 5 will require $2(UN_v)/(C_{max}+1)$ bit-level operations where C_{max} represents the value of the

maximum coefficient in the selected polynomial \bar{F}_W in (13) i.e the degree of polynomial \bar{F}_W . As an example, when $W = 9$, the value of C_{max} is 21.

Consider an implementation of both forms of binary sequences on a Texas Instruments (TI) TMS320C67x DSP [45] device. On this platform single precision (32-bit) floating point addition, subtraction and multiplication operations each take 5 clock cycles while floating point compare, fixed point unsigned integer addition and bit-wise logical operations are single cycle operations. Figure 6 shows graphs of the estimated number of total DSP clock cycles for CB and FB sequences (with W set to 9) as a function of various values of N_v when $U = 32$. Figure 6 indicates that FB sequences require significantly less DSP resources even for large values of N_v when compared to CB sequences.

6 Conclusions

A new form of binary SLM sequences obtained from a Fibonacci series and referred to as Fibonacci-Binary (FB) sequences has been proposed. Both CB and the proposed FB sequences have similar PAPR reduction performance when U is small and at higher CCDF

probability level. As U becomes larger and at lower CCDF level, CB sequences appear to produce slightly improved, but near comparable PAPR reduction performance, when compared to FB sequences. In the presence of some non-linear PA distortion i.e. IBO levels, both CB and the proposed FB sequences produce very similar BER performance for $U = 32$ despite the apparent small difference in their PAPR reduction performance. In terms of computational complexity, the construction of the proposed FB sequences requires significantly reduced numbers of DSP computations compared to CB sequences. Therefore, if the level of computational complexity is used as a criterion for SLM sequence selection, as may often be the case for practical systems, then the proposed FB sequences may be the preferred choice over CB sequences.

References:

- [1] S. Adegbite, B. Stewart, and S. McMeekin, "Least Squares Interpolation Methods for LTE System Channel Estimation over Extended ITU Channels," *International Journal of Information and Electronics Engineering*, vol. 3, no. 4, pp. 414–418, July 2013.
- [2] M. Mahmoud and M. Riad, "OFDM system under the combined effect analysis of the phase noise, carrier frequency offset, Doppler spread, and amplifier nonlinearity of the SEL," *WSEAS Trans. on Communications*, no. 7, pp. 719–728, 2008.
- [3] H. J. Taha and M. Salleh, "Multi-carrier transmission techniques for wireless communication systems: a survey," *WSEAS Transactions on Communications*, vol. 8, no. 5, pp. 457–472, 2009.
- [4] C. Sharma, S. K. Tomar, and A. Gupta, "PAPR reduction in OFDM system using adapting coding technique with pre distortion method," *WSEAS Trans. on Communications*, no. 9, pp. 255–262, 2011.
- [5] A. Vallavaraj, B. Stewart, D. Harrison, and F. McIntosh, "Reduction of Peak-to-Average Power Ratio of OFDM symbols using phasing schemes combined with companding," in *GCC Conference (GCC), 2006 IEEE*, March 2006, pp. 1–5.
- [6] J. Armstrong, "OFDM for Optical Communications," *Lightwave Technology, Journal of*, vol. 27, no. 3, pp. 189–204, 2009.
- [7] B. Stewart and A. Vallavaraj, "The Application of u-Law Companding to the WiMax IEEE802.16e Down-Link PUSC," in *Parallel and Distributed Systems, 2008. ICPADS '08. 14th IEEE International Conference on*, 2008, pp. 896–901.
- [8] K. Bae, C. Shin, and E. J. Powers, "Performance Analysis of OFDM Systems with Selected Mapping in the Presence of Nonlinearity," *Wireless Communications, IEEE Transactions on*, vol. 12, no. 5, pp. 2314–2322, 2013.
- [9] H.-S. Joo, S.-J. Heo, H.-B. Jeon, J.-S. No, and D.-J. Shin, "A New Blind SLM Scheme With Low Decoding Complexity for OFDM Systems," *Broadcasting, IEEE Transactions on*, vol. 58, no. 4, pp. 669–676, 2012.
- [10] S. H. Han and J. H. Lee, "An overview of peak-to-average power ratio reduction techniques for multicarrier transmission," *Wireless Communications, IEEE*, vol. 12, no. 2, pp. 56 – 65, April 2005.
- [11] T. Jiang and Y. Wu, "An Overview: Peak-to-Average Power Ratio Reduction Techniques for OFDM Signals," *Broadcasting, IEEE Transactions on*, vol. 54, no. 2, pp. 257–268, 2008.
- [12] D.-W. Lim, S.-J. Heo, and J.-S. No, "An overview of peak-to-average power ratio reduction schemes for OFDM signals," *Communications and Networks, Journal of*, vol. 11, no. 3, pp. 229–239, 2009.
- [13] A. Mobasher and A. Khandani, "Integer-based constellation-shaping method for PAPR reduction in OFDM systems," *Communications, IEEE Transactions on*, vol. 54, no. 1, pp. 119–127, 2006.
- [14] J. Armstrong, "Peak-to-average power reduction for OFDM by repeated clipping and frequency domain filtering," *Electronics Letters*, vol. 38, no. 5, pp. 246–247, 2002.
- [15] H. Ochiai and H. Imai, "Performance analysis of deliberately clipped OFDM signals," *Communications, IEEE Transactions on*, vol. 50, no. 1, pp. 89–101, 2002.
- [16] L. Wang and C. Tellambura, "A simplified clipping and filtering technique for PAR reduction

- in OFDM systems,” *Signal Processing Letters, IEEE*, vol. 12, no. 6, pp. 453–456, 2005.
- [17] R. Bauml, R. Fischer, and J. Huber, “Reducing the peak-to-average power ratio of multicarrier modulation by selected mapping,” *Electronics Letters*, vol. 32, no. 22, pp. 2056–2057, Oct. 1996.
- [18] S. Muller and J. Huber, “OFDM with reduced peak-to-average power ratio by optimum combination of partial transmit sequences,” *Electronics Letters*, vol. 33, no. 5, pp. 368–369, 1997.
- [19] E. Hassan, S. El-Khamy, M. Dessouky, S. El-Dolil, and F. El-Samie, “Peak-to-average power ratio reduction in space-time block coded multi-input multi-output orthogonal frequency division multiplexing systems using a small overhead selective mapping scheme,” *Communications, IET*, vol. 3, no. 10, pp. 1667–1674, 2009.
- [20] E. Hong, H. Kim, K. Yang, and D. Har, “Pilot-Aided Side Information Detection in SLM-Based OFDM Systems,” *Wireless Communications, IEEE Transactions on*, vol. 12, no. 7, pp. 3140–3147, 2013.
- [21] S. Adegbite, S. McMeekin, and B. Stewart, “Low-complexity data decoding using binary phase detection in SLM-OFDM systems,” *Electronics Letters*, vol. 50, no. 7, pp. 560–562, Mar. 2014.
- [22] A. Vallavaraj, B. Stewart, D. Harrison, and F. McIntosh, “Reducing the PAPR of OFDM Using a Simplified Scrambling SLM Technique with No Explicit Side Information,” in *Parallel and Distributed Systems, 2008. ICPADS '08. 14th IEEE International Conference on*, 2008, pp. 902–907.
- [23] E. Badran and A. El-Helw, “A Novel Semi-Blind Selected Mapping Technique for PAPR Reduction in OFDM,” *Signal Processing Letters, IEEE*, vol. 18, no. 9, pp. 493–496, 2011.
- [24] A. D. S. Jayalath and C. Tellambura, “SLM and PTS peak-power reduction of OFDM signals without side information,” *Wireless Communications, IEEE Transactions on*, vol. 4, no. 5, pp. 2006–2013, 2005.
- [25] J. Park, E. Hong, and D. Har, “Low Complexity Data Decoding for SLM-Based OFDM Systems without Side Information,” *Communications Letters, IEEE*, vol. 15, no. 6, pp. 611–613, 2011.
- [26] G. Zhou and L. Peng, “Optimality Condition for Selected Mapping in OFDM,” *Signal Processing, IEEE Transactions on*, vol. 54, no. 8, pp. 3159–3165, 2006.
- [27] C. Peng, X. Yue, D. Lilin, and L. Shaoqian, “Optimized phase sequence set for SLM-OFDM,” in *Communications, Circuits and Systems, 2007. ICCAS 2007. International Conference on*, 2007, pp. 284–287.
- [28] S. Boyd, “Multitone signals with low crest factor,” *Circuits and Systems, IEEE Transactions on*, vol. 33, no. 10, pp. 1018–1022, 1986.
- [29] M. Park, H. Jun, J. Cho, N. Cho, D. Hong, and C. Kang, “PAPR reduction in OFDM transmission using Hadamard transform,” in *Communications, 2000. ICC 2000. 2000 IEEE International Conference on*, vol. 1, 2000, pp. 430–433 vol.1.
- [30] N. Ohkubo and T. Ohtsuki, “Design criteria for phase sequences in selected mapping,” in *Vehicle Technology Conference, 2003. VTC 2003-Spring. The 57th IEEE Semi-annual*, vol. 1, 2003, pp. 373–377.
- [31] J. W. Cooley and J. W. Tukey, “An algorithm for the machine calculation of complex Fourier series,” *Mathematics of Computation*, vol. 19, no. 90, pp. 297–301, 1965.
- [32] S. Johnson and M. Frigo, “A Modified Split-Radix FFT With Fewer Arithmetic Operations,” *Signal Processing, IEEE Transactions on*, vol. 55, no. 1, pp. 111–119, 2007.
- [33] A. Peled and A. Ruiz, “Frequency domain data transmission using reduced computational complexity algorithms,” in *Acoustics, Speech, and Signal Processing, IEEE International Conference on ICASSP '80.*, vol. 5, Apr. 1980, pp. 964–967.
- [34] L. Yu, J. P. Barbot, G. Zheng, and H. Sun, “Compressive Sensing With Chaotic Sequence,” *Signal Processing Letters, IEEE*, vol. 17, no. 8, pp. 731–734, 2010.
- [35] A. Kurian, S. Puthusserypady, and S. M. Htut, “Performance enhancement of DS/CDMA system using chaotic complex spreading sequence,” *Wireless Communications, IEEE Transactions on*, vol. 4, no. 3, pp. 984–989, 2005.
- [36] C.-C. Chen, K. Yao, K. Umemo, and E. Biglieri, “Design of spread-spectrum sequences using

- chaotic dynamical systems and ergodic theory,” *Circuits and Systems I: Fundamental Theory and Applications, IEEE Transactions on*, vol. 48, no. 9, pp. 1110–1114, 2001.
- [37] N. Irukulapati, V. Chakka, and A. Jain, “SLM based PAPR reduction of OFDM signal using new phase sequence,” *Electronics Letters*, vol. 45, no. 24, pp. 1231–1232, Sept. 2009.
- [38] A. Goel, M. Agrawal, and P. G. Poddar, “M-ary Chaotic Sequence Based SLM-OFDM System for PAPR Reduction without side information,” *World Academy of Science, Engineering and Technology (WASET)*, vol. 68, no. 137, pp. 821–826, Aug. 2012.
- [39] S. Agaian, M.-C. Chen, and C. L. P. Chen, “Noise reduction algorithms using Fibonacci Fourier transforms,” in *Systems, Man and Cybernetics, 2008. SMC 2008. IEEE International Conference on*, 2008, pp. 1048–1052.
- [40] S. Nishihara and H. Nishino, “Binary Search Revisited: Another Advantage of Fibonacci Search,” *Computers, IEEE Transactions on*, vol. C-36, no. 9, pp. 1132–1135, 1987.
- [41] R. Stankovic, M. Stankovic, J. Astola, and K. Egiazarian, “Fibonacci decision diagrams and spectral Fibonacci decision diagrams,” in *Multiple-Valued Logic, 2000. (ISMVL 2000) Proceedings. 30th IEEE International Symposium on*, 2000, pp. 206–211.
- [42] Y. Guo and J. Cavallaro, “A novel adaptive pre-distorter using LS estimation of SSPA non-linearity in mobile OFDM systems,” in *Circuits and Systems, 2002. ISCAS 2002. IEEE International Symposium on*, vol. 3, 2002, pp. 453–456.
- [43] C. Rapp, “Effects of HPA nonlinearity on a 4-DPSK/OFDM signal for a digital sound broadcasting system,” in *Proc. 2nd European Conference on Satellite Communication, Liege, Belgium*, Oct. 1991, pp. 179–184.
- [44] M. Failli, “Digital land mobile radio communications COST 207,” ETSI, Tech. Rep., European Commission, 1989.
- [45] “Texas Instruments (TI): TMS320C67x/C67x+ DSP, CPU and Instruction Set Reference Guide,” Nov. 2006.